

Supplement of The Cryosphere, 12, 1401–1414, 2018
<https://doi.org/10.5194/tc-12-1401-2018-supplement>
© Author(s) 2018. This work is distributed under
the Creative Commons Attribution 3.0 License.



Supplement of

Accumulation patterns around Dome C, East Antarctica, in the last 73 kyr

Marie G. P. Cavitte et al.

Correspondence to: Marie G. P. Cavitte (mariecavitte@gmail.com)

The copyright of individual parts of the supplement might differ from the CC BY 3.0 License.

S1: Bed topography in the Dome C region

Figure S1 shows Bedmap2 topography with the Young et al. (2017) refined bed elevation grid obtained using the OIA survey radar data (outlined with a dashed rectangle). The surface contours highlight the areas of reduced surface slope. The same (small-scale) areas of higher accumulation discussed in the manuscript (Fig. 3, 5 and 6 of the manuscript) are highlighted here. The accumulation variations we observe are co-located with significant bedrock relief changes, which reach e.g. ~2000 m for the Concordia Ridge (CR) escarpment, and ~500 m for the south side of the Little Dome C Massif (LDCM).

10 S2: Reconstructed accumulation rate uncertainties

The calculated time-averaged accumulation rate (\bar{a}) uncertainties are plotted for the entire region in Fig. S2, and have an average value of 0.16 mm-we yr⁻¹. The Metropolis-Hastings (MH) iterations calculate a steady-state uncertainty which takes into account the age uncertainty of the radar isochrones. We first calculate depth uncertainties for all radar isochrones which take into account the range precision of the isochrones, the firm correction error and the radio-wave propagation uncertainty variation with depth. The age uncertainty of the radar isochrones is a combination of the radar depth uncertainties translated to an age uncertainty (Cavitte et al., 2016) and the AICC2012 ice core chronology uncertainties (Veres et al., 2013; Bazin et al., 2013). This uncertainty is obtained after 100 MH iterations, each taking 5 thermo-mechanical iteration (see companion paper, Parrenin et al., 2017). Parrenin et al. (2017) The calculated uncertainties are relatively small and uniform over the LDCM, remaining below 0.3 mm-we yr⁻¹. They more than double east of the CR, where the rough topography limits the applicability of the 1D pseudo-steady ice flow model. Additional error arising from assuming a constant ice thickness is not taken into account in these uncertainties. However, it does not affect the spatial distribution of accumulation uncertainties, but rather increases the magnitude of accumulation uncertainties uniformly for the entire Dome C region. If we include this additional 5% error on accumulation rates (see manuscript): the area east of the CR (where uncertainties are already highest) has a resulting rms error of 1.2 mm-we yr⁻¹. Compared to the small-scale accumulation rate variations observed which represent accumulation differences of ~5 mm-we yr⁻¹ (see Fig.3 of the manuscript), this source of error is negligible.

30 S3: Slope in the Prevailing Wind Direction (SPWD) in the Dome C region

Figure S3 shows surface slopes in the prevailing wind direction (SPWD) calculated from Bamber et al. (2009) surface topography and ECMWF 5-year average wind directions. Time-averaged accumulation rates \bar{a} as shown in Fig.3 of the main manuscript are plotted on top. We see that the small-scale areas of high accumulation observed are co-located with areas of markedly reduced

35 SPWD values with respect to the surrounding values ($\sim 1.2-1.5 \times 10^{-3}$ of SPWD change). This fits
well with the model put forward by Frezzotti et al. (2007) over Talos Dome where accumulation
increases when the SPWD decreases. We are only referring to the absolute magnitude of the SPWD
values as described in Frezzotti et al. (2007), but there is also an interesting polarity of the SPWD
40 values across the divide. The prevailing wind direction over the area is more or less along the long
axis of Dome C flowing from further up the ice divide towards Dome C (Frezzotti et al., 2005; Urbini
et al., 2008).

S4: Spatial anomaly of paleoaccumulation rates

We show the detrended paleoaccumulation rates for all four layers going back to 73 ka. The 0 -
10 ka interval is repeated from Fig.6 in the manuscript for comparison. Although the spatial extent
45 of layers older than 10 ka is reduced due to the filtering applied to remove regions of excess hori-
zontal strain, the small-scale areas of high accumulation appear to remain spatially stationary. High
detrended paleoaccumulation values are found where the surface curvature is strongly positive (i.e.
surface trough), and low values are found where the surface curvature is strongly negative (i.e. sur-
face bump). As the layers get older and deeper (reaching $\sim 30\%$ of the ice thickness for the 46 - 73
50 ka layer), this relationship gets increasingly offset in space due to increased amounts of horizontal
advection with depth (up to the set maximum of 5 km).

S5: Example radargram and isochrones

We show the detailed radargram along transect B-B' (OIA/JKB2n/Y77a) with and without isochrone
interpretations to show the quality of the radar data used in this study, and show the depth coverage
55 of the interpreted internal isochrones.

References

- Bamber, J., Gomez-Dans, J., and Griggs, J.: A new 1 km digital elevation model of the Antarctic derived from combined satellite radar and laser data—Part 1: Data and methods, *The Cryosphere*, 3, 101–111, doi:10.5194/tc-3-101-2009, 2009.
- 60 Bazin, L., Landais, A., Lemieux-Dudon, B., Toyé Mahamadou Kele, H., Veres, D., Parrenin, F., Martinerie, P., Ritz, C., Capron, E., Lipenkov, V., et al.: An optimized multi-proxy, multi-site Antarctic ice and gas orbital chronology (AICC2012): 120-800 ka, *Climate of the Past*, 9, 1715–1731, doi:10.5194/cp-9-1715-2013, 2013.
- 65 Cavitte, M. G., Blankenship, D. D., Young, D. A., Schroeder, D. M., Parrenin, F., Lemeur, E., Macgregor, J. A., and Siegert, M. J.: Deep radiostratigraphy of the East Antarctic plateau: connecting the Dome C and Vostok ice core sites, *Journal of Glaciology*, 62, 323–334, 2016.
- Fretwell, P., Pritchard, H. D., Vaughan, D. G., Bamber, J., Barrand, N., Bell, R., Bianchi, C., Bingham, R., Blankenship, D., Casassa, G., et al.: Bedmap2: improved ice bed, surface and thickness datasets for Antarctica, *The Cryosphere*, 7, 2013.
- 70 Frezzotti, M., Pouchet, M., Flora, O., Gandolfi, S., Gay, M., Urbini, S., Vincent, C., Becagli, S., Gragnani, R., Proposito, M., et al.: Spatial and temporal variability of snow accumulation in East Antarctica from traverse data, *Journal of Glaciology*, 51, 113–124, 2005.
- Frezzotti, M., Urbini, S., Proposito, M., Sarchilli, C., and Gandolfi, S.: Spatial and temporal variability of surface mass balance near Talos Dome, East Antarctica, *Journal of Geophysical Research: Earth Surface*, 112, 2007.
- 75 Parrenin, F., Cavitte, M. G. P., Blankenship, D. D., Chappellaz, J., Fischer, H., Gagliardini, O., Masson-Delmotte, V., Passalacqua, O., Ritz, C., Roberts, J., Siegert, M. J., and Young, D. A.: Is there 1.5-million-year-old ice near Dome C, Antarctica?, *The Cryosphere*, 11, 2427–2437, doi:10.5194/tc-11-2427-2017, <https://www.the-cryosphere.net/11/2427/2017/>, 2017.
- 80 Urbini, S., Frezzotti, M., Gandolfi, S., Vincent, C., Sarchilli, C., Vittuari, L., and Fily, M.: Historical behaviour of Dome C and Talos Dome (East Antarctica) as investigated by snow accumulation and ice velocity measurements, *global and planetary change*, 60, 576–588, 2008.
- Veres, D., Bazin, L., Landais, A., Toyé Mahamadou Kele, H., Lemieux-Dudon, B., Parrenin, F., Martinerie, P., Blayo, E., Blunier, T., Capron, E., et al.: The Antarctic ice core chronology (AICC2012): an optimized multi-parameter and multi-site dating approach for the last 120 thousand years, *Climate of the Past*, 9, 1733–1748, doi:10.5194/cp-9-1733-2013, 2013.
- 85 Young, D. A., Roberts, J. L., Ritz, C., Frezzotti, M., Quartini, E., Cavitte, M. G. P., Tozer, C. R., Steinhage, D., Urbini, S., Corr, H. F. J., van Ommen, T., and Blankenship, D. D.: High-resolution boundary conditions of an old ice target near Dome C, Antarctica, *The Cryosphere*, 11, 1897–1911, doi:10.5194/tc-11-1897-2017, <https://www.the-cryosphere.net/11/1897/2017/>, 2017.

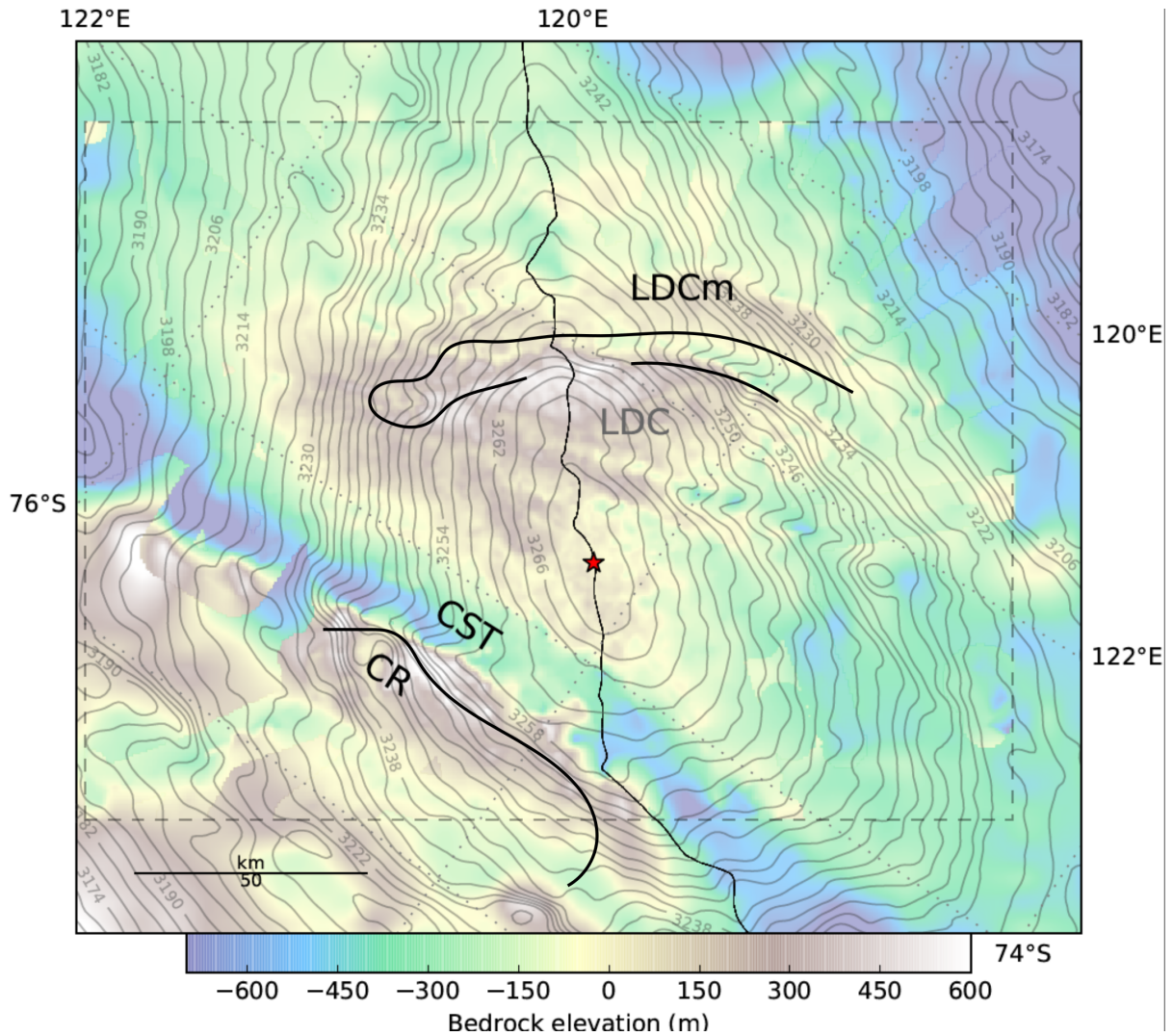


Figure S 1: Bedmap2 bedrock elevations (Fretwell et al., 2013) with recompiled OIA radar bed elevations (Young et al., 2017) delimited by a dashed rectangle. The same black lines highlighting the areas of small-scale high accumulation as on Fig.3 are drawn to highlight the influence of the bed on small-scale accumulation variations. Gray contours are Bamber et al. (2009) surface elevations, a black line locates the ice divide. A red star locates the EPICA Dome C ice core. LDC locates the gentle secondary surface dome, LDCM locates the Little Dome C massif under the densest radar lines, CR locates the Concordia Ridge steep escarpment along the Concordia Subglacial Trench (CST).

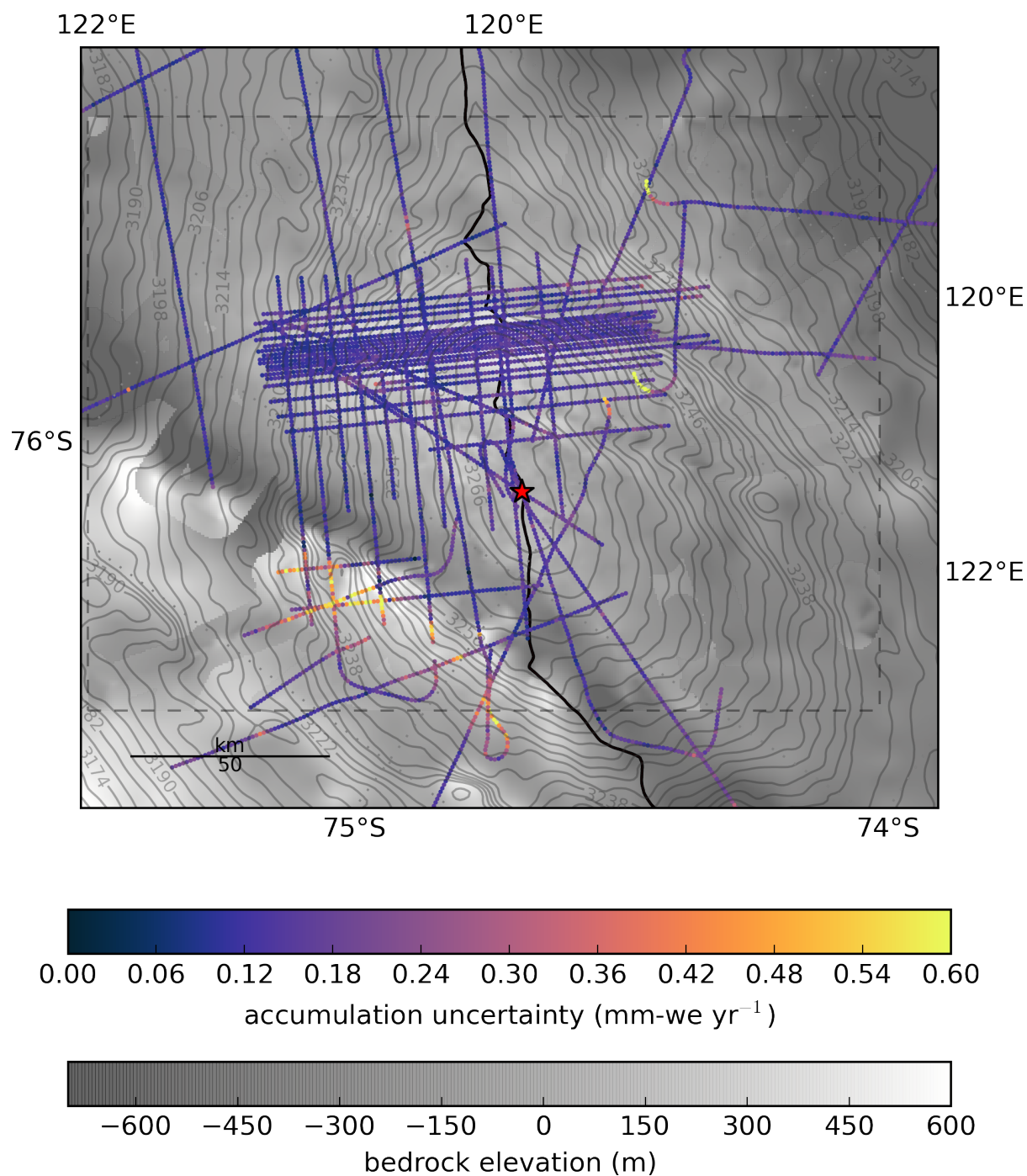


Figure S 2: Time-averaged accumulation rate uncertainties over the Dome C region. Uncertainties are low over the LDCM, but increase east of the CR area. Background is the same as in Fig. S1 in grayscale.

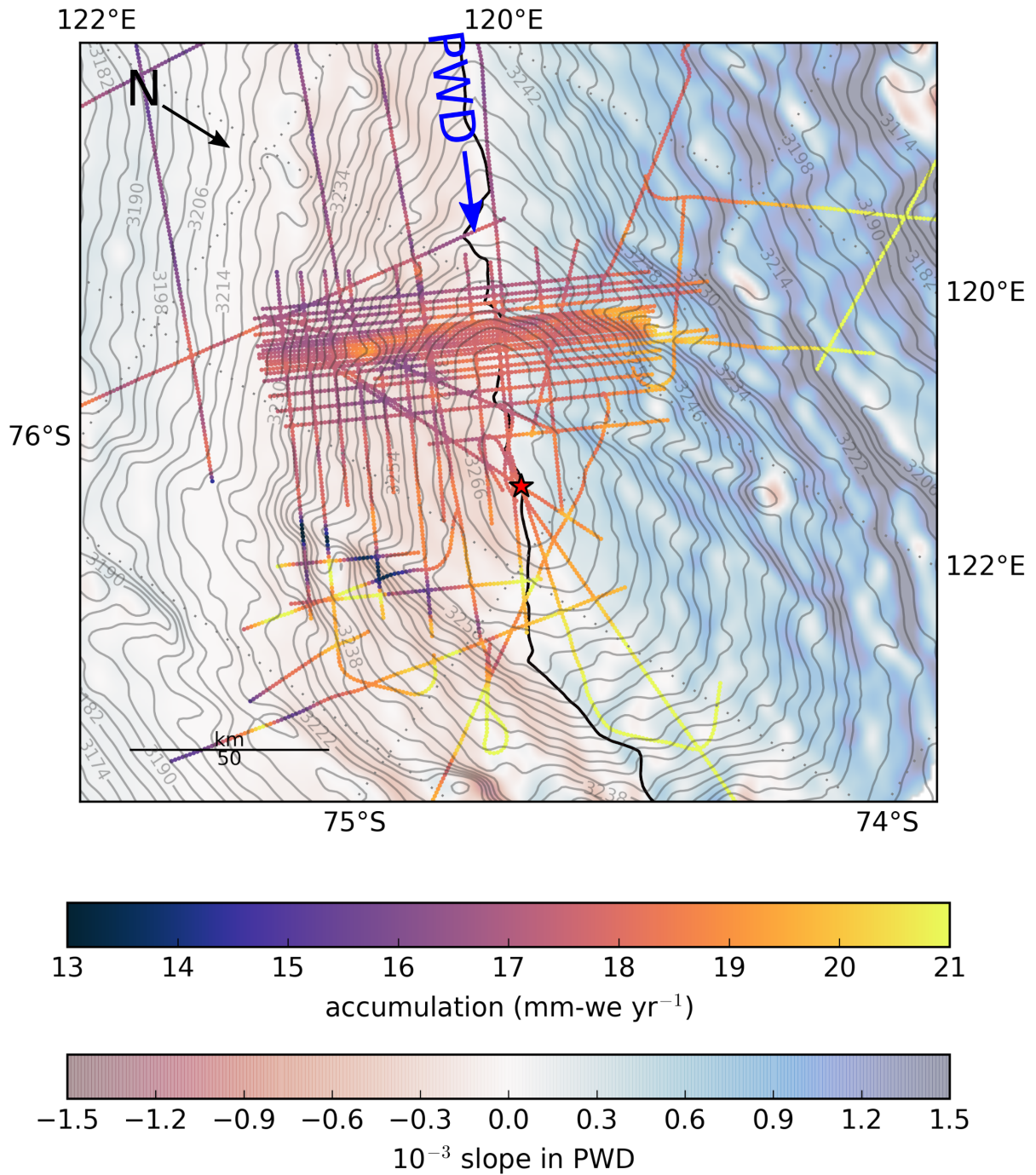


Figure S 3: Time-averaged accumulation rates \bar{a} over the Dome C region, overlain on surface slope in the prevailing wind direction (SPWD). The prevailing wind direction (PVD) is indicated by a blue arrow.

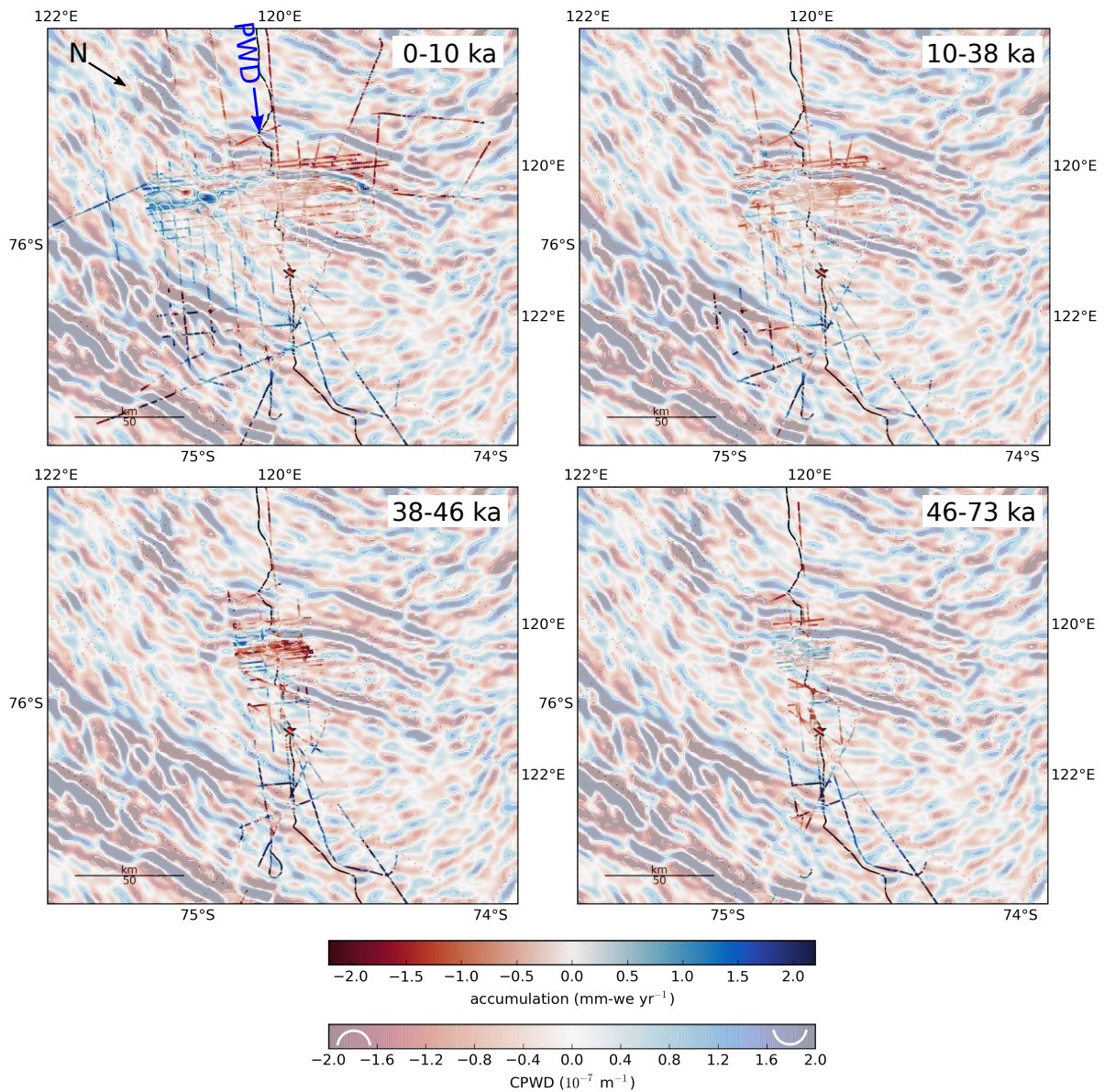


Figure S 4: Residual paleoaccumulations over the region, overlain on surface curvature in the prevailing wind direction (CPWD, strongly positive and negative values are sketched on either end of the colorbar). Panels show the same age intervals as Fig.4 and results are similarly filtered to remove regions of excess horizontal strain (see manuscript). The residual paleoaccumulation highs correlate well to areas of strongly positive CPWD. As layers get older, increasing offsets are visible east of the CR. A blue arrow indicates prevailing wind direction.

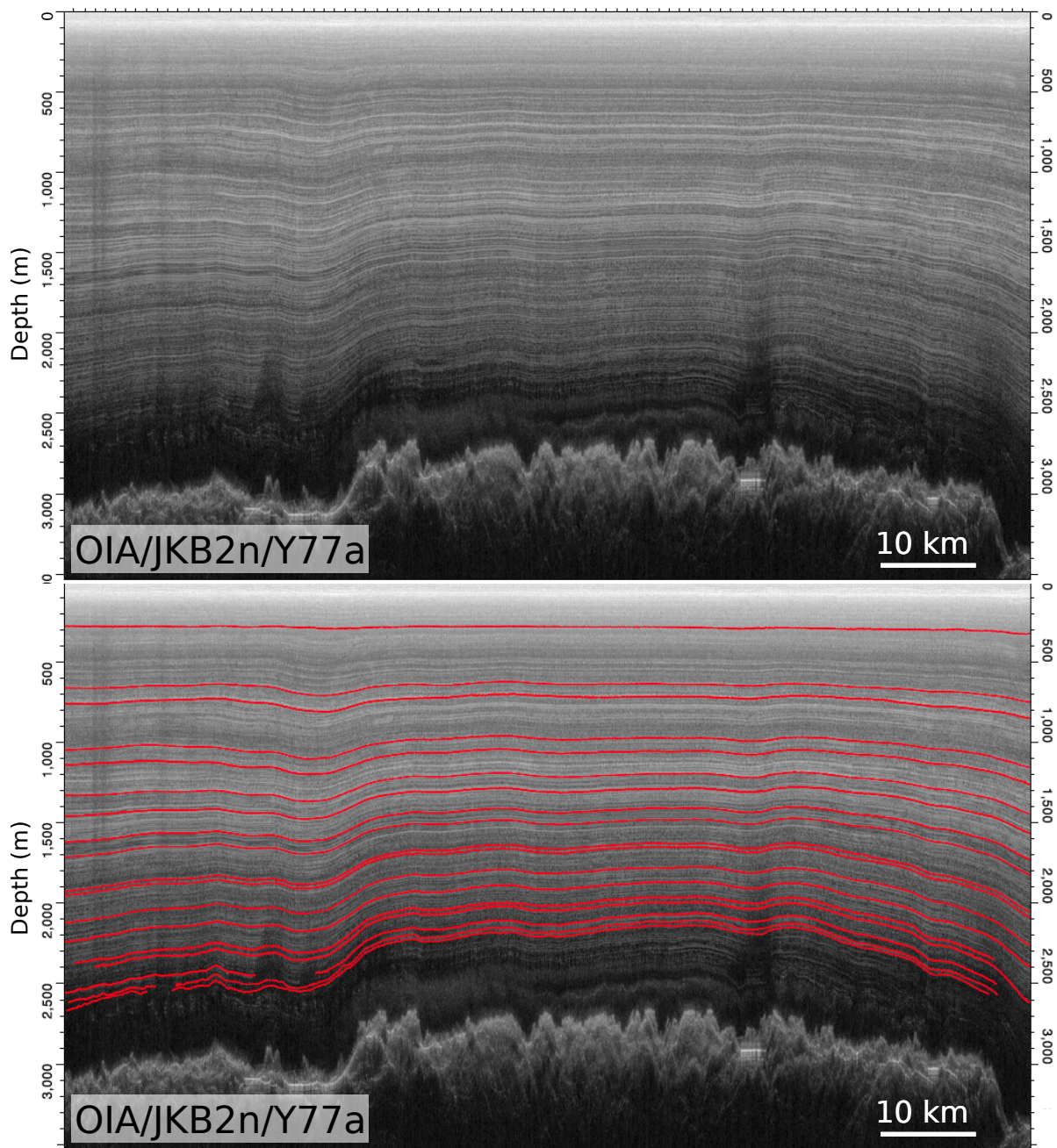


Figure S 5: Radargram along transect B-B' (OIA/JKB2n/Y77a). Upper panel shows the raw radargram, lower panel shows the interpreted internal isochrones overlain in red.